

Comparison of Crystal Structure between Low- and High-Temperature Phases of Diethyl (Z,Z)-muconate. A Trial to Investigate the Reasons Why the Solid-State Polymerization Reaction Is Ceased at Low Temperature

Seishi SARAGAI, Kohji TASHIRO,[†] Shinsuke NAKAMOTO, Toshiya KAMAE, Akikazu MATSUMOTO,* and Takashi TSUBOUCHI*

Department of Macromolecular Science, Graduate School of Science, Osaka University, Toyonaka, Osaka 560-0043, Japan

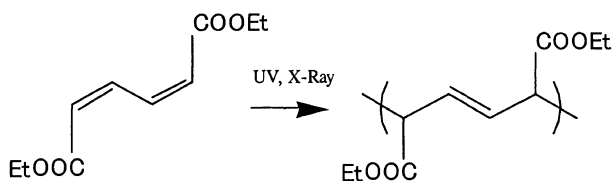
*Department of Applied Chemistry, Faculty of Engineering, Osaka City University, Sugimoto, Sumiyoshi-ku, Osaka 558-8585, Japan

(Received October 16, 2000; Accepted November 24, 2000)

ABSTRACT: Diethyl (Z,Z)-muconate (EMU) shows the topotactic polymerization reaction in the solid-state by an irradiation of light. This reaction occurs quite rapidly at room temperature but reduces its rate gradually at lower temperature and does not occur at all below -45°C , where the 1st-order phase transition occurs. In order to clarify the reasons why the reaction is ceased in the low-temperature phase, the X-Ray structural analysis was made at -80°C by using an imaging plate system. The molecular packing structure was found to be slightly different from that at room temperature. If the reactivity is affected quite sensitively by such a slight difference in packing structure, we have to say that the solid-state polymerization of EMU can be induced for the first time when the molecular packing mode satisfies the quite narrow and limited geometrical condition. But, this idea is difficult to be accepted at the present stage judging from the small structural difference between the two phases. As seen typically for the case of polydiacetylenes, the solid-state polymerization or in more general the topochemical reactions had been discussed so far in terms of such packing geometry as the inter-atomic distance, the molecular orientation in the crystal lattice, etc. But this rule is considered to be too simple to interpret the remarkable difference in the polymerization reactivity at high- and low-temperatures of EMU. In other words, this example of EMU brings up a very important warning about the conventionally-made discussion on the factors governing the solid-state polymerization reaction.

KEY WORDS Diethyl (Z,Z)-muconate / Topotactic Polymerization / Phase Transition / X-Ray Structure Analysis / Packing Geometry / Reactivity /

In the previous papers we have investigated the light-induced solid-state polymerization reaction of a series of (Z,Z)-muconate with the various side groups. Diethyl (Z,Z)-muconate (EMU: diethyl (Z,Z)-2,4-hexadienedioate) is one of the special cases in which the so-called topotactic polymerization reaction occurs in the solid-state with the single crystal morphology kept unchanged during the reaction.^{1–4}



We carried out the X-Ray structure analysis of the starting monomers by using a rapid-scan-type CCD camera system.⁵ The CCD camera system was used there because the polymerization reaction occurred too fast to be traced by the conventional X-Ray diffraction machine such as AFC (automatic four-circle X-Ray diffractometer) and Imaging Plate. As shown in Figure 1, the EMU molecules form the columnar structure and the polymerization reaction occurs along this columnar axis. The polymerization reaction occurs by forming the covalent CC bonds between the butadiene carbon atoms of the neighboring monomer molecules. The space group sym-

metry of the polymer crystal is the same with that of the monomer crystal, giving a strong evidence that this EMU exhibits the typical but very rare topotactic polymerization reaction.

The EMU monomer crystal shows the very rapid polymerization reaction at room temperature but the reaction rate decreases gradually as the temperature is decreased.^{2,3} In the DSC thermogram measured in a wide temperature region, a small endothermic peak is observed around -45°C .⁴ The X-Ray diffraction profile measured for the powdered sample changes remarkably at this transition point. The loss of the polymerization reactivity might be related with this remarkable change in the crystal lattice structure.

So far the relation between the crystal structure and the polymerization reactivity had been investigated by comparing the packing structures of the compounds of different chemical formulae, but the comparison between the different *crystal modifications* of the same chemical compound is the most useful and direct for this discussion. EMU might be one of the best candidates for this purpose. Therefore, in order to clarify the key factors governing the reaction mechanism of the solid-state polymerization of EMU, we need absolutely necessarily to analyze the crystal structure of the EMU monomer at the low temperature (the low-temperature phase) and to compare it with the structure at room temperature (the high-temperature phase).

Generally speaking the structure analysis of the crystal showing the phase transition at low temperature is

[†]To whom correspondence should be addressed.

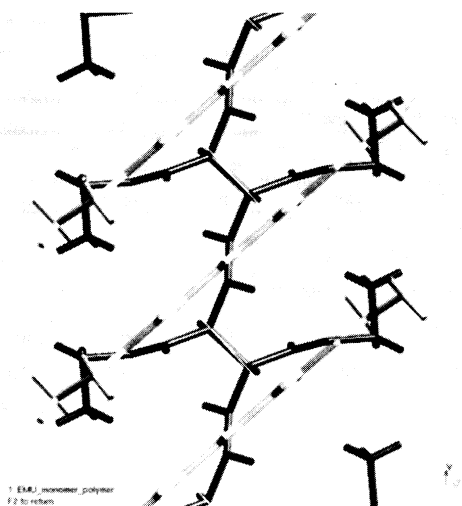


Figure 1. Comparison of packing structure of monomers and polymer in the crystal lattices analyzed before and after the polymerization reaction.⁵ By making a connection between the butadiene carbon atoms of the adjacent monomers (white thin lines), the new covalent bond is created to give the polymer chain.

difficult to make, because the crystal is cracked into the smaller mosaics by cooling. This cracking may occur even when the cooling rate is quite low so that the system experiences the transition almost quasi-statically. The case of EMU is not also an exception. After many times of failure, we could get an idea for this problem and carried out the X-Ray diffraction measurement successfully with almost no reduction of the quality of the reflection data.

In the present paper the result of the thus carried out structure analysis is reported and the comparison of the packing modes is made between the two crystal phases in order to get the useful factors governing the light-induced solid-state polymerization reaction.

EXPERIMENTAL

Samples

EMU molecules were synthesized starting from the (*Z*, *Z*)-2,4-hexadienedioic acid ((*Z*, *Z*)-muconic acid) supplied by Mitsubishi Chemicals Co. Ltd., Japan, by the method described in previous paper.² Single crystals were grown from the hexane solution by the solvent evaporation method at room temperature. Most of the thus prepared single crystals of needle shape were cracked easily by cooling below the phase transition temperature even when the cooling rate was quite slow. We thought that this cracking was caused by the heterogeneous shrinkage of the large single crystal due to the low thermal conductivity and the inhomogeneous blowing of the cooled nitrogen gas onto the sample. Therefore, it might be possible to keep the crystal from being cracked if the sample is cracked thoroughly and beforehand by cooling down to very low temperature and only one tiny single crystal is picked up and is supplied to the X-Ray diffraction measurement at low temperature. This small single crystal is expected not to be broken any more at low temperature because the sample may not be strained heterogeneously. Actually we could collect the sufficient num-

ber of X-Ray reflections of relatively high quality, which were necessary for the structure analysis, by using this type of crystal although the reflection intensities were much lower than the case of the sample of normal size. In order to avoid an occurrence of the light-induced reaction during the preparation of the samples, all the processes were made under a weak red lamp in the dark room.

X-Ray Measurement

The X-Ray diffraction data were collected by using an X-Ray imaging plate system DIP3000 (MAC Science Co. Ltd., Japan). As an incident X-Ray source the graphite-monochromatized Mo- K_{α} line ($\lambda = 0.71073 \text{ \AA}$) was used, which was generated from the SRA-M18XHF rotating anode X-Ray generator (50 kV and 200 mA). The data collection was performed by a commercial software XDIP (MAC Science Co. Ltd., Japan). The sample was oscillated in a range of 2° over a rotation angle of $0-180^{\circ}$ around the ω axis. The exposure time was 30 min for one frame of diffraction image. It took about 30 h to collect the 60 images in total. Measurements were carried out at -80°C using a Cryostream cooler (Oxford Cryosystem, UK) with liquid nitrogen as a coolant, where the temperature-controlled nitrogen gas was blown to the sample directly. Temperature fluctuation was about $\pm 0.5^{\circ}\text{C}$. Temperature was monitored by a thermocouple set at a position as close to the sample as possible.

Structural Analysis

The thus measured 2-dimensional diffraction images were analyzed by using the software DENZO and SCALEPACK.^{6,7} The DENZO indexed the observed reflections, and refined the lattice parameters and the geometrical parameters of the measurement system such as the rotational axis of the sample, the center position of the oscillation, etc. The SCALEPACK refined the lattice parameters and adjusted the intensity scale between the successive images, from which the exact structure factors were obtained. The crystal structure was solved by using the software maXus (Nonius BV, Delft, the Netherlands), which consisted of a set of software necessary for the determination of the space group symmetry and initial models, the least-squares refinement of these models, etc. The direct method was used to find out the initial models, where the software SIR 92 developed by Altmar *et al.* was used.⁸ Least squares refinement was made on the basis of the full matrix method by using the quantity $\sum w(|F_o|^2 - |F_c|^2)^2$ as a minimized function with the weight $w = \exp[FA \times \sin^2\theta/\lambda^2] / [\sigma^2(F_o) + FB \times F_o^2]$, where $\sigma^2(F_o)$ was the square standard deviation of the observed structure factor F_o and the coefficients FA and FB were set to the values 0.0 and 0.03, respectively. The reflections satisfying the cut-off condition of $|F_o| > 3\sigma(|F_o|)$ were used in the least squares refinement. Because no detectable effect was found actually, the absorption correction for the observed intensity was not included in the structural refinement. Finally obtained reliability factors, R and R_w , were defined by the following equations; $R = \sum ||F_o^2| - |F_c^2|| / \sum |F_o^2|$ and $R_w = [\sum w(|F_o^2| - |F_c^2|)^2 / \sum w|F_o^2|^2]^{1/2}$.

Table I. Crystallographic data of the low- and high-temperature phases of EMU

	Low-temp phase	High-temp phase
Crystal system	Monoclinic	Monoclinic
Space group	$P2_1/c-C_{2h}^5$	$P2_1/c-C_{2h}^5$
Unit cell ^d	$a = 10.412(17) \text{ \AA}$ $b = 4.253(3) \text{ \AA}$ $c = 12.172(22) \text{ \AA}$ $\beta = 103.821(80)^\circ$	$a = 10.232(2) \text{ \AA}$ $b = 4.931(1) \text{ \AA}$ $c = 11.497(3) \text{ \AA}$ $\beta = 107.146(10)^\circ$
Distance d_{CC} ^a	3.88 \AA	3.79 \AA
Tilting angle ϕ ^b	57°	49°
Distance d_{mm} ^c	4.25 \AA	4.93 \AA

^a The intermolecular distance between the butadiene carbon atoms of the neighboring molecules along the b -axis. ^b The tilting angle of the molecular axis from the columnar axis. ^c The distance between the centers of mass of the neighboring molecules along the b -axis. ^d The standard errors are indicated by parentheses behind the corresponding cell parameters. For example, 10.412 (17) means $10.412 \pm 0.017 \text{ \AA}$.

RESULTS AND DISCUSSION

Table I shows the crystallographic data of the low- and high-temperature phases of EMU. The reflections observed at -80°C for the low temperature phase of EMU crystal were indexed by a monoclinic unit cell with $a = 10.412 \pm 0.017 \text{ \AA}$, $b = 4.253 \pm 0.003 \text{ \AA}$, $c = 12.172 \pm 0.022 \text{ \AA}$, and $\beta = 103.821 \pm 0.080^\circ$. The space group is $P2_1/c-C_{2h}^5$ and the two molecules are included in this unit cell. Final reliability factors were $R = 0.129$ and $R_w = 0.145$. These values were not so small as the generally accepted ones (R and $R_w \leq 0.05$) because of the relatively low signal-to-noise ratio of the reflection data, coming from the appreciably severe measurement conditions. At the present stage it is actually the limitation because the sample was too small and had to be kept at low temperature for a long time and the X-Ray beam could not be increased much in order to keep the sample from being polymerized by the strong X-Ray beam. Besides, as described below, the obtained crystal structure is not unreasonable and can be considered to be used for the qualitative discussion, at least, of the structural difference between the high-temperature and low-temperature phases. The obtained packing structure of monomer molecules is shown in Figure 2. The fractional coordinates of the atoms are listed in Table II. The geometrical parameters of the molecule and the intermolecular nonbonded interatomic distances are listed in Table III, where the parameters are compared between the low- and high-temperature phases.

As seen in Table I, when the cell parameters are compared between these two phases, the b axial length parallel to the direction of the polymerization reaction is contracted by about 14% from the room temperature value. The a axial length is not changed so much. The c axial length is increased by ca. 6%, and the angle β changes by about 3° . The space group symmetry is not changed between these two phases. The molecular geometry of the low-temperature phase is also essentially the same with that of the high-temperature phase. In Figure 3 the packing structure of the monomer molecules in the low-temperature phase is compared with that of the high-temperature phase. The high-

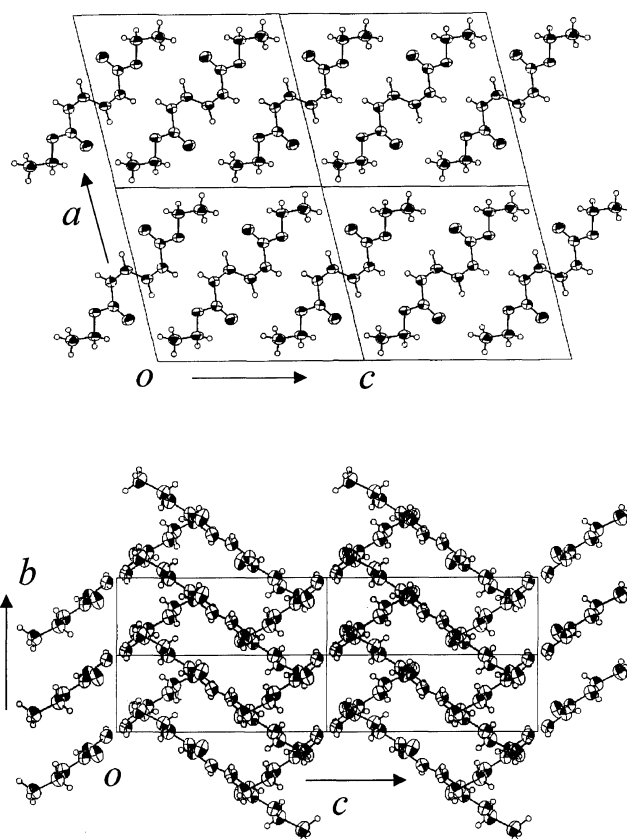
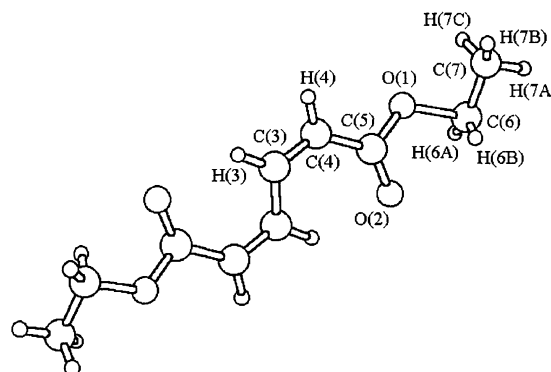


Figure 2. Crystal structure of the low-temperature phase of EMU. (upper) b -axis projection, and (lower) a -axis projection. Ellipsoid represents the anisotropic thermal parameter of each atom.

Table II. Fractional atomic coordinates and equivalent isotropic displacement parameters for diethyl (Z,Z)-muconate at -80°C

	x	y	z	$U_{eq} (\text{\AA}^2)^a$
O(1) ^b	0.2857(7)	0.0010(3)	0.2527(7)	0.0503(5)
O(2)	0.2428(1)	-0.2157(4)	0.4072(9)	0.0667(6)
C(3)	0.5260(1)	-0.4422(5)	0.4540(1)	0.0489(7)
C(4)	0.4590(1)	-0.2702(6)	0.3677(1)	0.0479(8)
C(5)	0.3194(1)	-0.1626(5)	0.3498(1)	0.0465(7)
C(6)	0.1490(1)	0.1150(5)	0.2235(1)	0.0528(7)
C(7)	0.1272(2)	0.2685(7)	0.1115(1)	0.0610(10)
H(3)	0.618(1)	-0.539(4)	0.451(1)	0.056(3)
H(4)	0.499(2)	-0.235(8)	0.311(1)	0.022(6)
H(6A)	0.091(2)	-0.085(8)	0.213(2)	0.076(6)
H(6B)	0.133(2)	0.222(6)	0.280(1)	0.073(5)
H(7A)	0.044(2)	0.331(5)	0.088(1)	0.046(4)
H(7B)	0.146(2)	0.133(7)	0.042(2)	0.064(5)
H(7C)	0.188(2)	0.407(6)	0.106(1)	0.048(5)

^a $U_{eq} = (1/3) \sum_j U_{ij} a_i a_j$. ^b The standard errors are indicated by parentheses behind the corresponding coordinates. The numbering of the atoms is shown below.



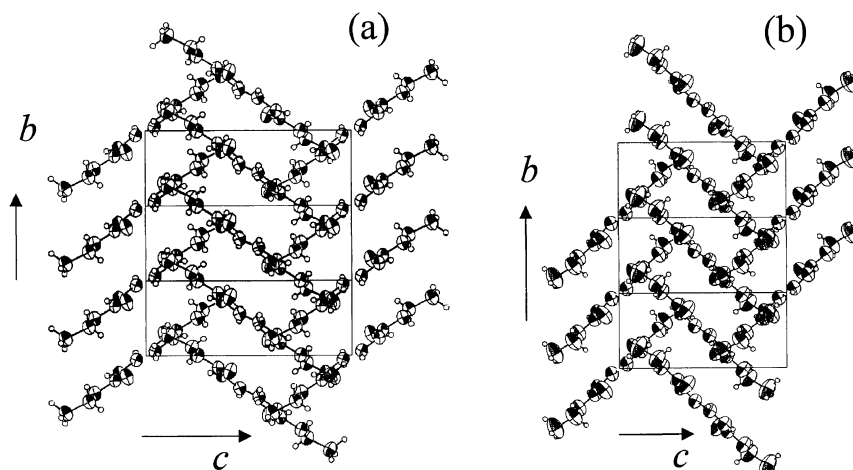


Figure 3. Comparison of packing structure of monomer molecules in (a) the low- and (b) the high-temperature phases of EMU (the a -axial projection). Both of the phases consist of the columns extending along the b -axis. Tilting angle of the molecular axis from the columnar axis is smaller in the low-temperature phase.

Table III. Selected geometric parameters (\AA , deg) for diethyl(Z,Z)-muconate at the low- and high-temperature phases

(A) Intramolecular bond length ^a		
	Low	High
O(1) - C(5)	1.344(2)	1.335(3)
O(1) - C(6)	1.465(2)	1.458(3)
O(2) - C(5)	1.201(2)	1.196(3)
C(3) - C(3')	1.442(3)	1.428(3)
C(3) - C(4)	1.332(3)	1.330(3)
C(4) - C(5)	1.489(3)	1.461(3)
C(6) - C(7)	1.479(3)	1.453(6)
(B) Intramolecular bond angles		
	Low	High
C(5) - O(1) - C(6)	114.8(1)	116.3(2)
C(3') - C(3) - C(4)	125.2(2)	127.1(2)
C(3) - C(4) - C(5)	126.4(2)	126.3(2)
O(1) - C(5) - O(2)	122.6(2)	122.6(2)
O(1) - C(5) - C(4)	109.2(2)	109.9(2)
O(2) - C(5) - C(4)	128.2(2)	127.4(2)
O(1) - C(6) - C(7)	107.2(2)	107.7(3)
(C) Intramolecular torsional angles		
	Low	High
C(6) - O(1) - C(5) - O(2)	-1.2(2)	-0.8(2)
C(6) - O(1) - C(5) - C(4)	-178.7(2)	-178.7(3)
C(5) - O(1) - C(6) - C(7)	176.1(2)	172.9(4)
C(3') - C(3) - C(4) - C(5)	-0.5(2)	0.0(2)
C(3) - C(4) - C(5) - O(1)	179.0(3)	179.1(3)
C(3) - C(4) - C(5) - O(2)	1.7(2)	1.3(3)
(D) Intermolecular non-bonded distances		
	Low	High
C(3) - C(4')	3.693(3)	3.930(3)
C(3) - C(5')	3.616(3)	3.709(3)
C(4) - C(4')	3.882(3)	3.791(3)
C(4) - C(5')	4.051(3)	3.871(3)
C(5) - C(6')	3.694(3)	3.994(4)
C(5) - C(7')	3.937(3)	3.959(5)

^a The numbering of the atoms is referred to in Tabel II. The standard errors are indicated by parentheses behind the corresponding internal coordinates.

temperature phase of EMU crystal can be polymerized quite rapidly and smoothly along the b axis or the column axis. As listed in Table I, the intermolecular distance (d_{CC}) between the butadiene carbon atoms of the neighboring molecules along the b axis is about 3.79 \AA and the tilting angle (ϕ) of the molecular axis from the columnar axis is about 49° . The distance between the centers of mass (d_{mm}) of the neighboring molecules along the b axis is 4.93 \AA . These structural situations may satisfy the conditions needed for inducing the effective and smooth polymerization reaction in the structurally-confined solid state. In the low-temperature phase, too, the molecules are packed in a column developed along the b axis as shown in Figure 2. As seen in Table I, the packing geometries such as ϕ , d_{CC} , and d_{mm} defined above are only slightly different from those of the high-temperature phase. In the previous paper,⁴ we reported the observation of small endothermic peak at *ca.* -45°C in the DSC thermogram of EMU crystal. Small difference in the packing mode of molecules in the high- and low-temperature phases may cause this small enthalpy change. It is a future problem to clarify what kinds of factor govern this thermal property or the phase transition behavior of EMU from the energetical point of view.

We have to remember here that the polymerization reaction does not occur at all below -45°C or the phase transition temperature. Therefore it is surprising for us to notice that only slightly different packing geometry of the molecules of almost the same shape gives the quite different behavior in the polymerization reaction. We have now the two different viewpoints. One is to accept this slight structural difference as the positive reasons for the large difference in the polymerization reaction. As discussed in a separate paper,⁹ the overlap of π -electron orbitals of the carbon atoms between the neighboring butadiene groups along the b axis seems important in the discussion of smooth propagation of the generated radicals along the columnar axis. The slight structural change might cause the change in the effective overlap of π -electron orbitals, resulting in the low reactivity in the low temperature region. Another viewpoint is to assume that the above-mentioned structural

difference is too small to cause the remarkable difference in the polymerization reaction. In fact, we investigated the crystal structure of a series of *Z,Z*-muconates diesters and compared the packing geometry between them.⁹ Some compounds show the *ZZ* to *EE* (or *cis,cis* to *trans,trans*) isomerization, and some other compounds give the polymers with irregular configuration. In spite of the large difference in the reaction behavior, they show the structural difference of the order comparable to that found for the two crystal phases of EMU as long as the above-mentioned three kinds of geometrical parameters (ϕ , d_{CC} , and d_{mm}) are concerned. In this way, if the geometrical difference between the low- and high-temperature phases of EMU can be assumed to be too small to give the reasonable explanation for the remarkable difference in the polymerization reactivity, we have to find the other factors which should control this difference.

As an important factor we must consider the thermal effect of the molecules. If the reaction is assumed to proceed kinetically by crossing some energy barrier from the starting monomer state to the reacted polymer (or oligomer) state, the polymerization reaction is speculated to become less active at low temperature, because the molecules may not very frequently cross this activation barrier. But this possibility cannot be adopted here, because we know one exceptional case of bis-*p*-bromobenzyl *Z,Z*-muconate which can be polymerized quite rapidly even at such a low temperature as -80°C .¹⁰

It is now very difficult to clarify the reasons for this reactivity difference on the basis of the simple comparison of the packing geometry. Some idea was proposed to interpret the difference in the polymerization reactivity of a series of polydiacetylene.¹¹ That is, only the monomer species, the geometry of which satisfies the very narrow range of the tilting angle ϕ and the distance d_{mm} between the adjacent monomers along the columnar axis, give the solid-state polymerization reaction. But, in this case of polydiacetylene, also, there are several exceptions, in which the packing geometry does not satisfy the above-mentioned conditions but gives very fast polymerization reaction. Therefore, it might be dangerous and

too early to give the conclusions about the factors governing the solid-state polymerization reaction of the present cases of muconates diester (and polydiacetylenes). We must emphasize here that the importance of the present study is in such a point that the comparison of the crystal structure between the low- and high-temperature phases of EMU could bring up one very important question about the discussion on the factors governing the polymerization reaction behavior of the monomer single crystals. In order to understand the real factors, it might be necessary to carry out the molecular orbital calculation of the excited molecular species and its reaction with the neighboring molecules in the crystal lattice, because the actual reaction should always be related with the excitation of the chemical species in the irradiation of light.

REFERENCES

1. A. Matsumoto, T. Matsumura, and A. Aoki, *J. Chem. Soc. Chem., Commun.*, 1389 (1994).
2. A. Matsumoto, T. Matsumura, and S. Aoki, *Macromolecules*, **29**, 423 (1996).
3. A. Matsumoto, K. Yokoi, S. Aoki, K. Tashiro, T. Kamae, and M. Kobayashi, *Macromolecules*, **31**, 2129 (1998).
4. K. Tashiro, T. Kamae, M. Kobayashi, A. Matsumoto, K. Yokoi, and S. Aoki, *Macromolecules*, **32**, 2449 (1999).
5. K. Tashiro, A. N. Zadorin, S. Saragai, T. Kamae, A. Matsumoto, K. Yokoi, and S. Aoki, *Macromolecules*, **32**, 7946 (1999).
6. Z. Otwinowski and W. Minor, "Methods in Enzymology in Macromolecular Crystallography: Part A", Ed., C. W. Carter, Jr. and R. M. Sweet, Academic Press, London, 1997, 276, p 307.
7. a) A. Otwinowski, in "Proceedings of the CCP4 Study Weekend: "Data Collection and Processing", Ed., L. Sawyer, N. Isaacs, and S. Bailey, SERC Daresbury Laboratory (England), 1993, p 56. b) W. Minor, "XDISPLAYF Program", Purdue University, 1993.
8. A. Altmare, G. Cascarano, C. Giacobozzo, A. Guagliardi, M. C. Burla, G. Polidori, and M. Camalli, *J. Appl. Crystallogr.*, **27**, 435 (1994).
9. K. Tashiro, S. Saragai, A. N. Zadorin, T. Kamae, S. Nakamoto, A. Matsumoto, K. Yokoi, and S. Aoki, *Polym. Prepr., Jpn.*, **47**, 3863 (1998).
10. A. Matsumoto, T. Tsubouchi, S. Saragai, and K. Tashiro, *Polym. Prepr. Jpn.*, **49**, 1173 (2000).
11. V. Enkelmann, *Adv. Polym. Sci.*, **63**, 91 (1984).